

# Natural Ordering and Uniform Tidal Effects in Globally Coupled Phase Oscillator Models

David Mertens

*Department of Physics and Astronomy, Dickinson College, Carlisle, Pennsylvania 17013, USA*

Globally coupled phase oscillator models, such as the Kuramoto model, exhibit spontaneous collective synchronization. Such models can be restated in terms of interactions within and between subsets of oscillators. An approximation for the internal structure of coherent subsets of oscillators can be made based on the observations of natural ordering and uniform tidal effects. The approximation is seen to perform well for predicting the microstructure in a variety of phase oscillator models.

Spontaneous collective synchronization among nearly identical phase oscillators is a classic emergent phenomenon and phase transition [1]. The first theoretical model to provide insight into this transition was provided by Winfree in 1967 [2] and takes the form

$$\dot{\theta}_i = \omega_i + \frac{K}{N} \sum_{j=1}^N P(\theta_j) Q(\theta_i). \quad (1)$$

The functions  $P$  and  $Q$  must be  $2\pi$ -periodic, and so can be expressed as trigonometric functions of angular differences and sums. Kuramoto considered a simpler coupling [3] given by:

$$\dot{\theta}_i = \omega_i + \frac{K}{N} \sum_{j=1}^N \Gamma(\theta_j - \theta_i). \quad (2)$$

The simplest coupling is  $\Gamma(\Delta\theta) = \sin(\Delta\theta)$ . Such a coupling tends to draw two nearby oscillators together, while the disorder in the natural rotation rates,  $\omega_i$ , tends to spread them out. For many choices of  $P$  and  $Q$  or of  $\Gamma$ , if the coupling  $K$  is strong enough and the variation of the  $\omega_i$  is small enough, a subset of the population will mutually entrain: they will lock into relative positions that are essentially fixed after an initial transient. Winfree argued that the fraction of mutually entrained oscillators exhibits a phase transition in the coupling  $K$ , and Kuramoto analytically calculated the magnitude of the entrained fraction for his model. Various models have been considered by other authors [4, 5] and together they have been used to describe the collective behavior of many physical systems including coupled Josephson junctions [6], laser arrays [7], electronic auto-oscillators [8], electrochemical oscillators [9, 10], and acoustically coupled mechanical rotors [11, 12].

Globally coupled phase oscillator models can be rewritten exactly as mean field models. Because of this, most research has focused on approximating the behavior of the mean field. The most important results are found with the approximation of large system size,  $N \rightarrow \infty$  [1, 13, 14]. Work focusing on finite populations relies on ensemble averaging to make any meaningfully general claims [15–17]. Unfortunately, the only published mechanism for elucidating population-specific tipping points is to measure or simulate the behavior directly.

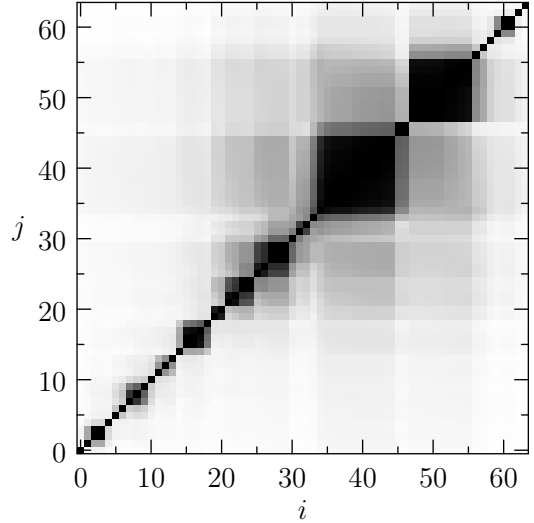


Figure 1: Pairwise correlations between all oscillators in a simulation of the Kuramoto model,  $N = 64$ . Lighter and darker intensity indicates smaller and larger values of  $\rho_{ij}$ , respectively. The indices were not optimized for block diagonal structure but were simply sorted according to  $\omega_i$ . For this simulation, the coupling strength is equal to the width of the population’s Gaussian distribution, placing it well below the critical coupling.

*Presence of coherent subsets* The mean field reformulation is exact, but it theoretically obscures an important observation. Figure 1 illustrates how groups of oscillators clump into groups (such as explored by Maistrenko et al. [18]). The intensity indicates the value of  $\rho_{ij}$ , defined as

$$\rho_{ij} e^{i\Delta_{ij}} \equiv \frac{1}{T} \int_0^T e^{i(\theta_i - \theta_j)} dt, \quad (3)$$

using  $i \equiv \sqrt{-1}$ . The obvious block diagonal structure is obtained simply by sorting the indices according to natural frequency  $\omega_i$ . Subsets of oscillators with nearby natural frequencies mutually entrain. Although not indicated in this figure, oscillators in these clumps also appear to act in concert, suggesting that their degrees of freedom are not independent. Taken together, these observations indicate that finite-sized phase oscillator models exhibit rich internal structure.

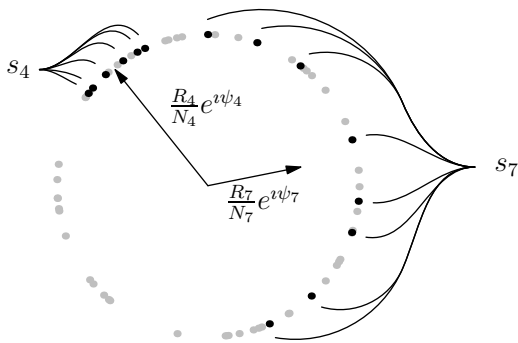


Figure 2: Depiction of two subsets (black dots) in a full population (black and gray dots) of 64 oscillators, not related to the simulation in figure 1. Subset 7 is more spread out than subset 4, and so has a smaller mean field relative to subset size. If these subsets are coherent, their constituent oscillators may get further apart or closer together, but they do not lap each other.

The presence of coherent subsets gives rise to a number of interesting questions. How do we best quantify the behavior of these coherent subsets? What approximations must be made to express the dynamics of the model in terms of the subsets' dynamics? How do the subsets evolve? Can we approximate the structure or evolution of the subsets? All of these questions will be addressed in this letter.

*Subset reformulation* The first papers on synchronization established that globally coupled phase oscillator models can be written exactly in terms of mean fields [2, 3]. For models with coupling that depends only on the first harmonic, such as the Kuramoto model, we use the mean field

$$r e^{i\psi} \equiv \frac{1}{N} \sum_{j=1}^N e^{i\theta_j}. \quad (4)$$

(Models that use the  $h^{th}$  harmonic need to consider the mean field defined using  $e^{ih\theta_j}$ .) By a trick of complex algebra[1], the dynamics of an individual oscillator can be exactly rewritten in terms of interactions with the mean field. For the Kuramoto model, the interactions take the form

$$\dot{\theta}_i = \omega_i + r K \sin(\psi - \theta_i). \quad (5)$$

If one could predict the behavior of  $r$  and  $\psi$ , one would essentially solve the dynamics of the Kuramoto model and could predict the properties of interest for the system. Ott and Antonsen provide a method for performing such a calculation for the Kuramoto model under the assumption of a continuous oscillator density [14]. Unfortunately, there is no generic closed form solution for  $r(t)$  or  $\psi(t)$  for an arbitrary *finite* population behaving according to the Kuramoto model or other similar models.

How might we improve upon the mean-field reformulation for finite sized systems? Consider the following

minor refinement: split the summation of the traditional order parameter into  $\mathcal{N}$  pieces:

$$\sum_{j=1}^N e^{i\theta_j} = \sum_{j \in s_1} e^{i\theta_j} + \sum_{j \in s_2} e^{i\theta_j} + \dots + \sum_{j \in s_{\mathcal{N}}} e^{i\theta_j}. \quad (6)$$

In this expression, the  $i^{th}$  oscillator's contribution  $e^{i\theta_i}$  occurs only once on the left and right; that is, each oscillator is assigned to only one subset,  $s_\ell$ . The assignment of oscillator  $\theta_i$  to subset  $s_\ell$  is (for the moment) arbitrary [21]. Taking a cue from the traditional analysis, define the *subset mean field* for the  $\ell^{th}$  subset as

$$R_\ell e^{i\psi_\ell} \equiv \sum_{j \in s_\ell} e^{i\theta_j}. \quad (7)$$

Two such subsets, along with their mean fields, are depicted in figure 2. Employing the geometric interpretation of complex numbers, we see that  $\psi_\ell$  points roughly to their average phase. If a subset's oscillators are near to each other then  $R_\ell \approx N_\ell$  and if they are scattered about the unit circle then  $R_\ell \ll N_\ell$ . The subset's mean field serves as a simple measure of the coherence and location of the subset, and its formulation emerges from the original order parameter definition.

The traditional order parameter can be calculated, without any approximations, in terms of these mean fields. A simple algebraic substitution leads to

$$r e^{i\psi} = \frac{1}{N} \sum_{\ell=1}^{\mathcal{N}} R_\ell e^{i\psi_\ell}. \quad (8)$$

The behavior of each oscillator can also be written exactly in terms of interactions with these mean fields. The specifics depend upon the functions  $P$  and  $Q$  in equation 1 or  $\Gamma$  in equation 2, but such a restatement can be obtained in terms of the harmonic mean fields after employing the proper trigonometric identities. For example, the oscillator dynamics for the Kuramoto model are

$$\dot{\theta}_i = \omega_i + \frac{K}{N} \sum_{\ell=1}^{\mathcal{N}} R_\ell \sin(\psi_\ell - \theta_i), \quad (9)$$

which closely resembles the mean-field interaction given in equation 5. Again, this equation does not rely on any approximations. The only limitation is that I have yet to predict  $R_\ell$  and  $\psi_\ell$ .

In order to predict the behavior of the subset mean fields, we need an expression for their dynamics. Evaluating the time derivative of the definition (equation 7) and rearranging leads to

$$\dot{R}_\ell + i\dot{\psi}_\ell R_\ell = \sum_{j \in s_\ell} i\dot{\theta}_j e^{i(\theta_j - \psi_\ell)} \quad (10)$$

$$= \sum_{j \in s_\ell} \dot{\theta}_j \sin(\psi_\ell - \theta_j) + i \sum_{j \in s_\ell} \dot{\theta}_j \cos(\psi_\ell - \theta_j). \quad (11)$$

The real and imaginary components give separate equations for the evolution of a subset amplitude and phase, respectively. To obtain the equations for a specific model,  $\dot{\theta}_j$  must be replaced with the expression for the time derivative specific to that model. Although the dynamics in  $\dot{\theta}_j$  depend upon all of the mean fields, judicious use of trigonometric identities can lead to separable contributions for internal dynamics and interactions between subset mean fields. The internal dynamics are of particular interest: if these could be approximated in terms of the subset's mean field, it would be possible to coarse-grain the dynamics of the oscillator model into a model for interacting amplitude oscillators representing the subsets. Such a coarse graining relies upon a good approximation for  $\psi_\ell - \theta_j$ .

*Coherent subset approximation* One good approximation for  $\psi_\ell - \theta_j$  that is independent of model details is the *coherent subset approximation*. The approximation is built on two observations about the clumps discussed on the first page:

1. Natural ordering: For oscillators in a coherent subset, the positions  $\theta_i$  order according to increasing natural speed,  $\omega_i$ .
2. Uniform tidal effects: Relative oscillator positions fluctuate *nearly in unison*. For oscillators in a coherent subset  $\ell$ , relative positions can be related to the subset's mean field amplitude,  $R_\ell$ .

While uniform tidal effects have not previously been noted, evidence of natural ordering is abundant in the literature, beginning with Winfree's discussion of syntalans in his original paper on the topic [2]. One mathematical approximation that reflects these two observations is

$$\theta_j - \psi_\ell \approx C (\omega_j - \bar{\omega}_\ell)^\alpha (N_\ell - R_\ell)^\beta. \quad (12)$$

The  $\omega$ -dependence reflects the observation of natural ordering. The dependence on the subset's mean field amplitude and the neglect of other time dependence reflects the observation of uniform tidal effects.

In the simplest calculation, the constant  $C$  and exponents  $\alpha$  and  $\beta$  *do not depend* on the details of the phase oscillator model, but only on the definition of the subset mean field. With a small rearrangement, equation 7 becomes

$$R_\ell = \sum_{j \in s_\ell} e^{i(\theta_j - \psi_\ell)}. \quad (13)$$

To obtain constraints on the constant and exponents, expand the real and imaginary components of equation 13 to second order in  $\theta_j - \psi_\ell$ . The imaginary component gives

$$\begin{aligned} 0 &= \sum_{j \in s_\ell} \sin(\theta_j - \psi_\ell) \\ &\approx C (N_\ell - R_\ell)^\beta \sum_{j \in s_\ell} (\omega_j - \bar{\omega}_\ell)^\alpha, \end{aligned} \quad (14)$$

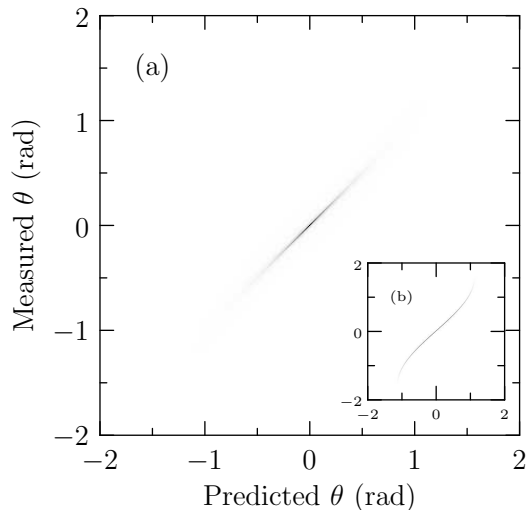


Figure 3: Histogram of actual (y) vs predicted (x) relative phase positions for the approximation given by equations 16 for the Kuramoto model. Intensity is linear in density. Figure (a) shows results for small subsets, each of which constitute fewer than 10% of their simulation's population. Figure (b) shows results for large subsets, each of which have more than 10% of their simulation's population. The data represent aggregated results of many simulations with a variety of coupling strengths and full population sizes, and with emergent subsets of various sizes. The correlation between the prediction and the measurement is  $r^2 = 0.86$  for (a),  $r^2 = 0.99$  for (b).

which can only hold generically if  $\alpha \equiv 1$ . The real component gives

$$\begin{aligned} R_\ell &= \sum_{j \in s_\ell} \cos(\theta_j - \psi_\ell) \\ &\approx N_\ell - \frac{C^2}{2} (N_\ell - R_\ell)^{2\beta} \sum_{j \in s_\ell} (\omega_j - \bar{\omega}_\ell)^{2\alpha}, \end{aligned} \quad (15)$$

which implies  $\beta = 1/2$  and  $C^{-2} = \frac{1}{2} \sum_{j \in s_\ell} (\omega_j - \bar{\omega}_\ell)^2 \equiv \Delta_\ell^2$ . Finally we arrive at

$$\theta_j - \psi_\ell \approx \frac{\omega_j - \bar{\omega}_\ell}{\Delta_\ell} \sqrt{N_\ell - R_\ell}, \quad (16)$$

This equation is the key result of this letter. Notice that the derivation does not rely on a particular form of  $P$ ,  $Q$ , or  $\Gamma$ . Although this equation does not predict which oscillators will aggregate into coherent subsets, it gives a model-independent time-dependent prediction for the steady-state structure of such subsets.

*Agreement with simulation* The agreement between the actual relative phases for the Kuramoto model and the predictions of equation 16 is shown in the density plots given in figure 3 and its inset. The main figure represents data from small subsets while the inset represents data from large subsets. The figure includes data from many different empirically identified subsets, them-

selves constituents of about 80 unrelated unimodal populations of various sizes, and all simulated with five coupling strengths. The coupling strengths are chosen randomly between 0 and 2; the critical coupling strength for these simulations is roughly 1.6 [1]. Additional details as well as other phase oscillator models are discussed in the supplementary material.

Figure 3 illustrates a strong correlation between the measurement and prediction: the approximation works well. Other models, such as the Ariaratnam-Strogatz model [4] or a third harmonic approximation to the sawtooth function, exhibit equally impressive small-subset results. The prediction is not perfect, with nonlinearities particularly prominent in the inset at large relative positions. It is perhaps unsurprising that large-subset data exhibit model-specific nonlinearities: these agree with the predictions of Sakaguchi and Kuramoto [5]. It is remarkable, however, that the nonlinearities are one-to-one. This one-to-one nature strongly suggests that more accurate predictions can be expressed as model-specific power series of equation 16. In other words, for models that exhibit natural ordering and uniform tidal effects, equation 16 serves as a universal starting point.

*Discussion and conclusion* The coherent subset approximation differs from similar results in the literature in key ways. Sakaguchi and Kuramoto predicted entrained relative phases for their model in ref [5] equation 5a. Their predictions only applied to oscillators entrained to the order parameter whereas equation 16 describes all coherent behavior, whether the mean field is appreciable or negligible, and whether or not the oscillators of interest are entrained to the mean field. It also gives a prediction for the instantaneous relative position which does not rely on long-time averaging or the coupling strength. Others have predicted the oscillator density distribution,  $\rho(\theta, \omega, t)$ , for the Kuramoto model with infinite system size and various population distributions [13, 14, 19]. Equation 16 is distinct from those predictions by addressing finite-size synchronization for a broad set of models, and by imposing no restriction on the population distribution. The coherent subset approximation is both more precise and more general than previous predictions.

The coherent subset approximation provides a new angle for analyzing distributions with finite support. In their impressive analysis, Martens et al. analytically compute nearly all of the bifurcation diagram for the Ku-

ramoto model with a Lorentzian bimodal frequency distribution [20]. As explained in the supplementary material, obtaining the saddle-node infinite-period (SNIPER) bifurcation curve for small  $\tilde{\sigma}$  is simple using the coherent subset approximation, and leads to unexpected scaling. Martens predicted that  $\tilde{\sigma} \propto 2 - \tilde{\omega}_0$  as  $\tilde{\omega}_0 \rightarrow 2$ . The coherent subset approximation, on the other hand, predicts that  $\tilde{\sigma} \propto \sqrt{2 - \tilde{\omega}_0}$  as  $\tilde{\omega}_0 \rightarrow 2$ . The range of values over which the scaling takes this form is not yet clear, but it should hold for any sufficiently narrow distribution with finite support. Whether an infinite bimodal Gaussian distribution would have linear or square-root scaling is intriguing but unknown.

All globally coupled phase oscillator models can be decomposed. The evolution of the subset mean fields is given by equation 11, even those models which do not exhibit natural ordering and uniform tidal effects. Unfortunately, the mean field dynamics given by equation 11 depend on model-specific details and so do not coarse grain to a universal form. If universality exists across a broad set of phase oscillator models, it will arise because the statistics of the aggregations do not depend upon the underlying model. This work provides the basis for such an analysis, but any such claims go beyond the scope of this letter.

In this letter, I have shown that the dynamics of globally coupled phase oscillator models can be restated exactly in terms of interactions among and within subsets. Phase oscillator models that exhibit natural ordering and uniform tidal effects will exhibit coherent subsets they have nearly identical microstructure. The approximation given in equation 16 appears to perform well and could serve as a starting point for more accurate approximations in a wide variety of models. Rather than relying on long-time or ensemble averaging to make meaningful predictions, an analysis based on subsets provides a formulation for predicting features of individual populations, paving the way for insights into a decades old problem in dynamic phase transitions.

### Acknowledgments

I would like to thank Georgios Tsekenis for fruitful discussion and insightful feedback during the preparation of this paper.

- 
- [1] S. Strogatz. From Kuramoto to Crawford: exploring the onset of synchronization in populations of coupled oscillators. *Physica D*, 143(1):1–20, 2000.
  - [2] Arthur T. Winfree. Biological rhythms and the behavior of populations of coupled oscillators. *Journal of Theoretical Biology*, 16(1):15–42, July 1967.
  - [3] Y. Kuramoto. Self-entrainment of a population of coupled nonlinear oscillators. volume 39 of *Lecture Notes in*

*Physics*, page 420. Springer-Verlag, 1975.

- [4] Joel Ariaratnam and Steven Strogatz. Phase Diagram for the Winfree Model of Coupled Nonlinear Oscillators. *Physical Review Letters*, 86(19):4278–4281, May 2001.
- [5] Hidetsugu Sakaguchi and Yoshiki Kuramoto. A soluble active rotator model showing phase transitions via mutual entrainment. *Prog. Theor. Phys.*, 76(3):576–581, September 1986.

- [6] Kurt Weisenfeld, Pere Colet, and Steven H. Strogatz. Frequency locking in Josephson arrays: Connection with the Kuramoto model. *Phys. Rev. E*, 57(2):1563–1569, February 1998.
- [7] S. Yu Kourtchatov, V. V. Likhanskii, A. P. Napartovich, F. T. Arecchi, and A. Lapucci. Theory of phase locking of globally coupled laser arrays. *Phys. Rev. A*, 52(5):4089–4094, November 1995.
- [8] Amirkhan A. Temirbayev, Zeinulla Zh. Zhanabaev, Stanislav B. Tarasov, Vladimir I. Ponomarenko, and Michael Rosenblum. Experiments on oscillator ensembles with global nonlinear coupling. *Physical Review E*, 85(1):015204, January 2012.
- [9] István Z. Kiss, Yumei Zhai, and John L. Hudson. Emerging Coherence in a Population of Chemical Oscillators. *Science*, 296(5573):1676–1678, April 2002.
- [10] István Z. Kiss. Resonance clustering in globally coupled electrochemical oscillators with external forcing. *Physical Review E*, 77(4), April 2008.
- [11] David Mertens and Richard Weaver. Synchronization and stimulated emission in an array of mechanical phase oscillators on a resonant support. *Physical Review E*, 83(4):046221, April 2011.
- [12] David Mertens and Richard Weaver. Individual and collective behavior of vibrating motors interacting through a resonant plate. *Complexity*, 16(5):45–53, 2011.
- [13] Juan A. Acebrón, Luis López Bonilla, Conrad J. Pérez Vicente, Félix Ritort, and Renato Spigler. The kuramoto model: A simple paradigm for synchronization phenomena. *Reviews of modern physics*, 77(1):137, 2005.
- [14] Edward Ott and Thomas M. Antonsen. Low dimensional behavior of large systems of globally coupled oscillators. *Chaos: An Interdisciplinary Journal of Nonlinear Science*, 18(3):037113, 2008.
- [15] H. Daido. Intrinsic Fluctuation and Its Critical Scaling in a Class of Populations of Oscillators with Distributed Frequencies. *Prog. Theor. Phys.*, 81(4):727–731, April 1989.
- [16] Choi Chulho, Ha Meesoon, and Byungnam Kahng. Extended finite-size scaling of synchronized coupled oscillators. *Phys. Rev. E*, 88:032126–1–032126–7, September 2013.
- [17] Michael A. Buice and Carson C. Chow. Correlations, fluctuations, and stability of a finite-size network of coupled oscillators. *Physical Review E*, 76(3):031118, 2007.
- [18] Yu. Maistrenko, O. Popovych, O. Burylko, and P. A. Tass. Mechanism of Desynchronization in the Finite-Dimensional Kuramoto Model. *Physical Review Letters*, 93(8):084102, August 2004.
- [19] D. Iatsenko, S. Petkoski, P. V. E. McClintock, and A. Stefanovska. Stationary and Traveling Wave States of the Kuramoto Model with an Arbitrary Distribution of Frequencies and Coupling Strengths. *Physical Review Letters*, 110(6):064101, February 2013.
- [20] E. Martens, E. Barreto, S. Strogatz, E. Ott, P. So, and T. Antonsen. Exact results for the Kuramoto model with a bimodal frequency distribution. *Physical Review E*, 79(2), February 2009.
- [21] Most of what I have to say about subset decomposition holds for any random decomposition, and can even be generalized to fractional and complex or imaginary membership.

## I. NUMERICAL SETUP

For all simulations, the population is sampled from a normal distribution of width  $\sigma = 1\text{rad}/s$  and mean  $\bar{\omega} = 1\text{rad}/s$ . The mean is inconsequential for the Kuramoto model but matters for one of the models considered below. In all simulations, I choose positions that are randomly distributed around the unit circle. The number of oscillators for a given simulation is sampled randomly from the uniform distribution between 30 and 5000.

I choose  $K$  values randomly from the uniform distribution between 0 and 2. Other models use other ranges as detailed below. The coupling ranges are based on trial and error, aiming to get a good sampling of unsynchronized and synchronized behavior for each model.

In all simulations presented, I follow the well-established practice of using a fourth-order Runge-Kutta method with a time step of 0.01s [1]. Based on the numerical evidence of Chulho et al. [1], the transient behavior of the Kuramoto model lasts for about  $3\sqrt{N_{osc}}$  seconds. I run all simulations for  $900\sqrt{N_{osc}}$  seconds, i.e. 30 multiples of the transient duration, storing the order parameter and oscillator positions each second, i.e. every 100 time steps. I then use the Mean Squared Error Rule to identify when the order parameter reaches steady state [2], using either that or  $3\sqrt{N_{osc}}$  seconds, whichever is larger.

## II. IDENTIFYING ENTRAINED SUBSETS OF OSCILLATORS

In addition to the order parameter and oscillator positions, I also monitor the phase differences between oscillators with consecutive natural speeds, and make note of all  $2\pi$  phase slips and the time step at which they occur. To identify coherent subsets, discard all phase slips that occur before the onset of the steady state and identify all pairs with *no* slips for the duration of the steady state. Such pairs are assumed to be mutually entrained. If one oscillator is entrained to two other oscillators, then all three of them must be mutually entrained. Using this approach, I extract the entrained subsets empirically.

## III. PRODUCING THE THIRD FIGURE

To produce the third figure in the letter, I select 1000 random moments in time,  $t_n$ , during the steady-state of each subset. I compute the subset mean field,  $R_\ell(t_n) e^{i\psi_\ell(t_n)}$ , from the  $\theta_j(t_n)$ . I then compute the actual relative position,  $\theta_j(t_n) - \psi_\ell(t_n)$ , as well as

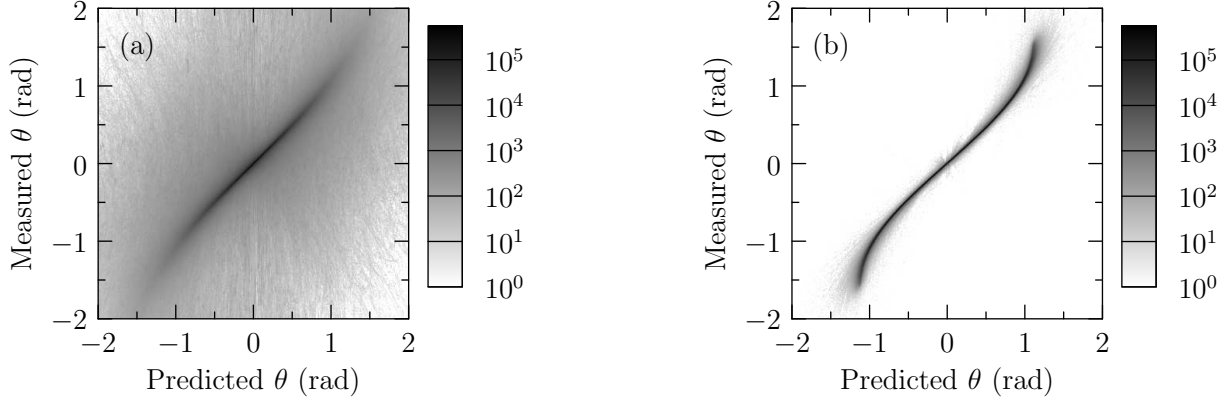


Figure 1: Prediction vs simulation for the Kuramoto model. Figure (a) is for small coherent subsets while figure (b) is for large coherent subsets. In contrast to the figure in the letter, the intensity indicates the logarithm of the density, rather than the density itself.

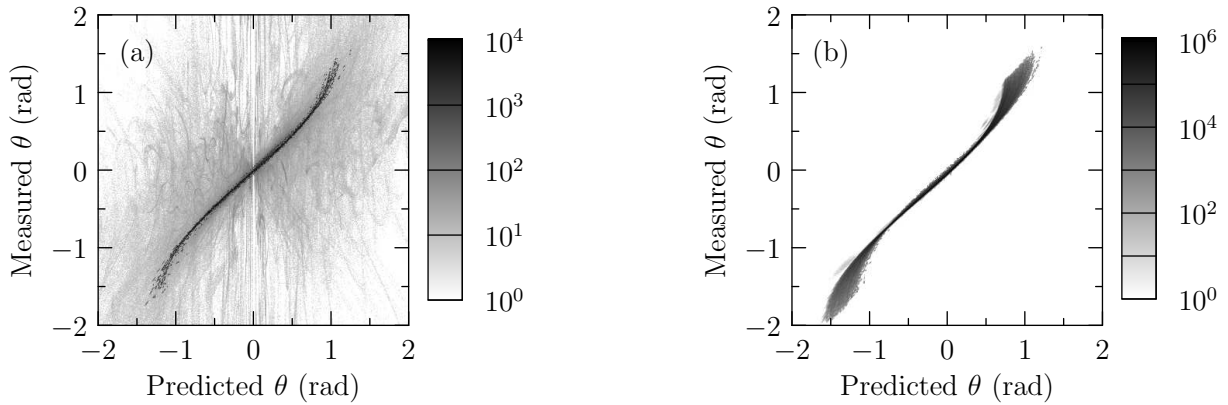


Figure 2: Prediction vs simulation for the Ariaratnam-Strogatz model, a Winfree model. Figure (a) is for small coherent subsets while figure (b) is for large coherent subsets. The correlation for the small subsets is  $r^2 = 0.99$  and for the large subsets is  $r^2 = 0.99$ .

the prediction for the relative positions based on  $R_\ell(t_n)$ . The plots are two-dimensional histograms depicting the number of times a predicted value of  $\theta_j - \psi_\ell$  for any one oscillator corresponded with any measured value of  $\theta_j - \psi_\ell$ .

#### IV. ADDITIONAL MODELS

In this section I present the results of the Kuramoto model alongside the results of two other globally coupled phase oscillator models.

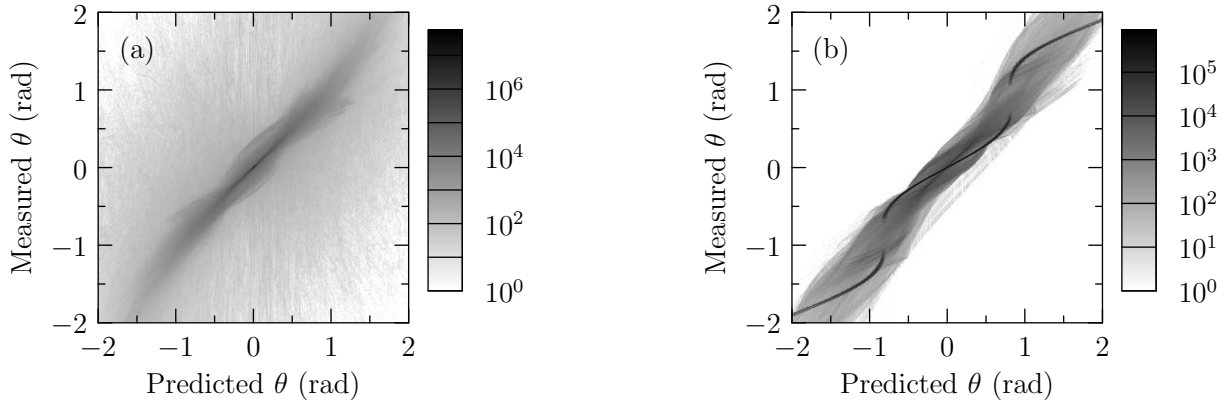


Figure 3: Prediction vs simulation for the third-harmonic sawtooth model, a Kuramoto-like model. Figure (a) is for small coherent subsets while figure (b) is for large coherent subsets. The correlation for the main figure is  $r^2 = 0.86$  and for the inset is  $r^2 = 0.95$ .

Figure 1 shows the small and large histograms for the Kuramoto model, using the same data as in the letter. In contrast to the figures in the main letter, the intensity indicates the logarithm of the density. This is necessary to represent the results of the sawtooth model, discussed below. Even with heightened sensitivity to small densities, the interpretation remains the same: relative positions are well approximated by the coherent subset approximation for small subsets, and one-to-one nonlinearities arise for large subsets.

Ariaratnam and Strogatz [3] considered a Winfree model for which  $P(\theta_j) = -1 - \cos\theta_j$  and  $Q(\theta_i) = \sin\theta_i$ . Figure 2 shows the small and large subset histograms for the model. For these simulations, the coupling was chosen randomly from the uniform distribution between 0 and 1. Strong correlations and nonlinear effects occur for subsets greater than 3% of the full population size, substantially smaller than for the Kuramoto model.

Note that the mean frequency is significant in this model. This model can be interpreted as a Kuramoto-like model in which the oscillators feel a pull between a “uniform field” directed toward  $\theta = 0$  coupled with strength  $K$ , a mean field coupled with strength  $K/2$ , and an odd additive term— $\sin(\theta_i + \theta_j)$ —also coupled with strength  $K/2$ . We expect the mean field to have two elements: a component aligned to the uniform field, and a component rotating in spite of the uniform field. Large  $\bar{\omega}$  should lead to more oscillators in the rotating component. Ariaratnam and Strogatz considered an evenly spaced distribution of oscillators, without disorder, so it is not known exactly how the choice of  $\bar{\omega}$  will effect the results, but an effect is expected.



The final model is a Kuramoto-like model based on the Fourier expansion of the sawtooth function truncated at the third harmonic, for which  $\Gamma(\Delta\theta) = \sin \Delta\theta - \frac{1}{2} \sin 2\Delta\theta + \frac{1}{3} \sin 3\Delta\theta$ . The results for this model are shown in figure 3. The coupling was chosen randomly from the uniform distribution between 0 and 4. The cutoff for large subsets was empirically set at 45%, substantially larger than for the Kuramoto model. It is also notable that the vast majority of the small-subset density lies within very small relative angles.

As mentioned in the main text, the predictions work fairly well, and although nonlinearities are present, the predictions still seem to have a one-to-one mapping to the measurements for most data. It is particularly interesting to note that large subset nonlinearities for the Kuramoto and the third-order sawtooth closely resemble the actual form of the coupling functions themselves!

## V. SQUARE-ROOT SCALING OF THE SNIPER BIFURCATION CURVE

In this section I will obtain a finite-size correction to the phase diagram of Martens et al [4]. To begin, I insert the form of  $\dot{\theta}_j$  from the Kuramoto model into equation 11 in the letter. I also substitute the coherent subset approximation, equation 16 in the letter, and expand the trigonometric sums to second order to obtain

$$\dot{R}_\ell = -2 \Delta_\ell \sqrt{N_\ell - R_\ell} + 2(N_\ell - R_\ell) \frac{K}{N} \sum_m R_m \cos(\psi_m - \psi_\ell), \quad (1)$$

$$\dot{\psi}_\ell R_\ell = \bar{\omega}_\ell R_\ell + (2R_\ell - N_\ell) \frac{K}{N} \sum_m R_m \sin(\psi_m - \psi_\ell). \quad (2)$$

For a symmetric bimodal population, for which all the oscillators are members of one of two coherent subsets  $s_1$  or  $s_2$ , I can obtain an expression for the mean field amplitudes  $R_1 = R_2 \equiv R_\ell$  as well as the difference of the phases,  $\Delta\psi \equiv \psi_2 - \psi_1$ :

$$\dot{R}_\ell = -2\Delta_\ell \sqrt{N_\ell - R_\ell} + 2(N_\ell - R_\ell) \frac{K}{N} R_\ell (1 + \cos \Delta\psi), \quad (3)$$

$$\frac{d}{dt} \Delta\psi = \bar{\omega}_2 - \bar{\omega}_1 - 2 \frac{2R_\ell - N_\ell}{N} K \sin \Delta\psi. \quad (4)$$

Now suppose that the peaks of the bimodal distribution are very narrow with respect to the coupling strength and their separation. In that case, the oscillators belonging to each peak should mutually entrain, behaving like two giant oscillators. The saddle-node infinite-period (SNIPER) bifurcation separates the the phase space where these two giant oscillators

are locked together or are counter-propagating. The dynamics for the locked oscillators are simply the fixed points given by  $\dot{R}_\ell = 0$  and  $\frac{d}{dt}\Delta\psi = 0$ , so

$$2\Delta_\ell\sqrt{N_\ell - R_\ell} = 2(N_\ell - R_\ell)\frac{K}{N}R_\ell(1 + \cos\Delta\psi), \quad (5)$$

$$\bar{\omega}_2 - \bar{\omega}_1 = 2\frac{2R_\ell - N_\ell}{N}K\sin\Delta\psi. \quad (6)$$

The saddle-node boundary occurs at values of  $\Delta_\ell$  and  $\bar{\omega}_2 - \bar{\omega}_1$  at which these equations can not be satisfied. The most extreme separation between  $\bar{\omega}_2 - \bar{\omega}_1$  occurs when  $\sin\Delta\psi \approx 1$ , in which case  $\cos\Delta\psi \approx 0$ , leading to

$$2\Delta_\ell\sqrt{N_\ell - R_\ell} = 2(N_\ell - R_\ell)\frac{K}{N}R_\ell, \quad (7)$$

$$\bar{\omega}_2 - \bar{\omega}_1 = 2\frac{2R_\ell - N_\ell}{N}K. \quad (8)$$

To obtain expressions using the notation of Martens, use

$$\bar{\omega}_2 - \bar{\omega}_1 = 2\omega_0, \quad (9)$$

$$\Delta_\ell^2 = \frac{N_\ell - 1}{2}\sigma_\ell^2. \quad (10)$$

Substituting this into the above expressions and eliminating  $R_\ell$  leads to

$$\frac{4\sigma_\ell}{K} = \frac{1}{4}\sqrt{2 - \frac{4\omega_0}{K}}\left(2 + \frac{4\omega_0}{K}\right)\sqrt{\frac{2N}{N-2}}. \quad (11)$$

Taking the large  $N$  limit so that  $N/(N-2) \approx 1$ , and using Martens' definitions,

$$\tilde{\sigma} = \frac{4\sigma_\ell}{K}, \quad (12)$$

$$\tilde{\omega}_0 = \frac{4\omega_0}{K}, \quad (13)$$

I obtain

$$\tilde{\sigma} = \frac{\sqrt{2}}{4}\sqrt{2 - \tilde{\omega}_0}(2 + \tilde{\omega}_0). \quad (14)$$

In contrast, in the vicinity of  $\tilde{\omega}_0 \approx 2$ , Martens' eq 33 comes to

$$\tilde{\Delta} = \frac{4}{7}(2 - \tilde{\omega}_0), \quad (15)$$

where  $\Delta$  represents the half-width-half-maximum of the individual peaks and  $\tilde{\Delta} \equiv 4\Delta/K$ .

I observed in the previous section that the coherent subset approximation is not exact for large separations  $\psi_\ell - \theta_j$ . These inconsistencies limit the range of applicability of my

calculation, but do not invalidate it. For subsets with sufficiently narrow  $\tilde{\sigma}$ , all relative positions should fall within the well-fit range of the prediction. The square-root dependence will certainly hold for these distributions.

---

- [1] Choi Chulho, Ha Meesoon, and Byungnam Kahng. Extended finite-size scaling of synchronized coupled oscillators. *Phys. Rev. E*, 88:032126–1–032126–7, September 2013.
- [2] Jr. White, K.P., M.J. Cobb, and S.C. Spratt. A comparison of five steady-state truncation heuristics for simulation. In *Simulation Conference, 2000. Proceedings. Winter*, volume 1, pages 755–760 vol.1, 2000.
- [3] Joel Ariaratnam and Steven Strogatz. Phase Diagram for the Winfree Model of Coupled Non-linear Oscillators. *Physical Review Letters*, 86(19):4278–4281, May 2001.
- [4] E. Martens, E. Barreto, S. Strogatz, E. Ott, P. So, and T. Antonsen. Exact results for the Kuramoto model with a bimodal frequency distribution. *Physical Review E*, 79(2), February 2009.